ChemComm

Accepted Manuscript

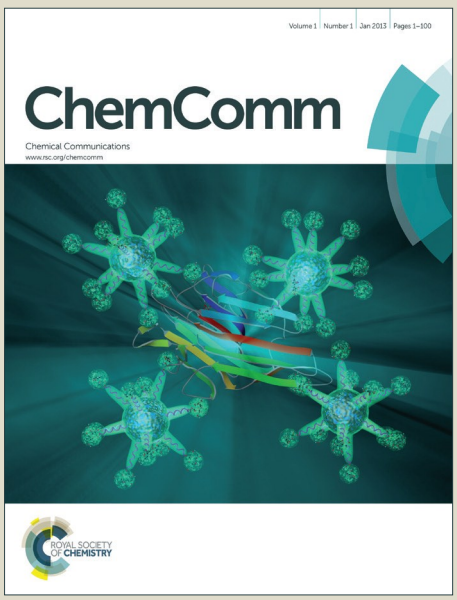

ROYAL SOCIETY OF CHEMISTRY

www.rsc.org/chemcomm

Journal Name

RSCPublishing

COMMUNICATION

Magnetic metal-organic framework nanocomposites for enrichment and direct detection of small molecules by negative-ion matrix-assisted laser desorption/Ionization time-of-flight mass spectrometry†

Cite this: DOI: 10.1039/x0xx00000x

Received 00th January 2012,
Accepted 00th January 2012

DOI: 10.1039/x0xx00000x

www.rsc.org/

Zian Lin,[ab] Wei Bian,[a] Jiangnan Zheng,[b] and Zongwei Cai[a]*

Zeolitic imidazolate framework-8 coated magnetic nanocomposites (Fe_3O_4@ZIF-8 MNCs) were served as absorbent and matrix for negative-ion MALDI-TOF MS. The host-guest property and interference-free background made it an ideal dual platform for the sensitive analysis of small molecules.

Matrix-assisted laser desorption/ionization time-of-flight mass spectrometry mass spectrometry (MALDI-TOF MS) has been used extensively for protein analysis.[1] However, analysis of small molecules by MALDI-TOF MS remains a challenge, due to the background interference of conventional organic matrices that can suppress and overlap with the analyte signals in the low mass region (<500 Da).[2] In addition, MALDI-TOF MS has the disadvantages of rather poor reproducibility, mainly originating from heterogeneity of the matrix-analyte crystals (so call "sweet spots"), which leads to MALDI-MS being heavily criticized for its quantitative analysis.

To overcome these drawback, an attractive method so called "surface-assisted laser desorption/ionization mass spectrometry (SALDI-MS)" has been developed by using nanomaterials as matrices.[3] Up to now, a variety of nanomaterials with different composition and morphology, including porous silicon,[4] metal/metal oxide nanoparticles,[5] and carbon-based materials,[6] have been successfully utilized as SALDI matrices. Although these methods have achieved some success, most development of nanomaterial-based matrices was accordingly based on the MS detection platform of positive ion mode, which often resulted in multiple sodium or potassium adducts in addition to protonated ions. Theoretically, the negative ion spectrum is much clearer and easier to interpret with only one deprotonated ion peak present.[7] Recent works also supported that negative ion MS can offer higher sensitivity than positive ion mode for analytes such as amino acids and peptides.[6b,c] Therefore, exploring new matrices for negative ion MALDI-MS is highly desirable.

Porous metal-organic frameworks (MOFs) have attracted immense attention in analytical science, because of their unique properties such as high porosity, large surface areas, and tunable pore sizes.[8] Especially, MOFs can provide high absorption capability in the UV-visible range, and thus meet the requirements to serve as SALDI matrices. Recently, an encouraging breakthrough in the utilization of MIL-100(Fe) MOFs as matrix was achieved by Huang's group,[8c] who reported the analysis of polycyclic aromatic hydrocarbons (PAHs) by positive ion MALDI-TOF MS. However, the general applicability and the advantages of MOFs as matrices for negative ion MALDI-TOF MS have not been demonstrated yet. Zeolitic imidazolate frameworks (ZIFs), as a new subfamily of MOFs, have gained particular interest due to their exceptional chemical and thermal stabilities.[9] 2-methylimidazole (HMeIM), as the major component of ZIF-8, possesses sp^2 hybridized nitrogen, which acted as Lewis base and tends to capture protons from the analytes upon their desorption. Consequently, ZIF-8 was supposed to accelerate the negative-charged process and yield abundant negative ions in negative ion mode.[6b] On the other hand, doping magnetic nanoparticles into MOFs is an effective way to tailor the magnetic property of MOFs, which exerts considerable effects on the applications of MOFs in sample pretreatment.[10] In principle, by virtue of the unique properties of MOFs and the magnetic property of Fe_3O_4 nanoparticles, the magnetic ZIF composites can be expected as an ideal absorbent and matrix for SALDI-MS. However, there is no report on the study of the magnetic ZIF-8 composites as matrix in MS technology.

Herein, ZIF-8 coated magnetic nanocomposites (Fe_3O_4@ZIF-8 MNCs) were synthesized by a facile approach and then for the first time served as matrix for negative ion MALDI-TOF MS. A comparison of Fe_3O_4@ZIF-8 with organic matrices revealed that the Fe_3O_4@ZIF-8 MNCs in negative ion mode can

a. Partner State Key Laboratory of Environmental and Biological Analysis, Department of Chemistry, Hong Kong Baptist University, 224 Waterloo Road, Kowloon Tong, Hong Kong, SAR, P. R. China

b. Ministry of Education Key Laboratory of Analysis and Detection for Food Safety, College of Chemistry, Fuzhou University, Fuzhou, Fujian, 350116, China

E-mail: zwcai@hkbu.edu.hk (Z.W.Cai)

Electronic Supplementary Information (ESI) available: See DOI: 10.1039/c000000x/

provide enhanced signal intensity, good salt tolerance and free matrix background in the analysis of small molecules. In addition, the Fe_3O_4@ZIF-8 MNCs served as an affinity probe for trace histidine (His) concentration and direct ionization in SALDI-MS were also discussed in this work.

The Fe_3O_4@ZIF-8 MNCs were synthesized at room temperature by using Fe_3O_4 as magnetic core, Zn^{2+} ion as connector and HMeIM as linker, which has been reported previously.[10b] Details of material synthesis and characterization were described in ESI†. Fig.1A shows the SEM image of the Fe_3O_4@ZIF-8 MNCs with good monodispersity and its average particle size was ~190 nm. TEM image (Fig.1B) clearly presented the core-shell structure of Fe_3O_4@ZIF-8 MNCs with ZIF-8 thicknesses (~25 nm). As shown in Fig.1C, the Fe_3O_4@ZIF-8 MNCs were well dispersed in ethanol/H_2O and its suspension exhibited strong absorption around 430 nm, which made it absorb laser energy and transfer energy to analyte possible. Generally, the best MALDI performance is achieved only at certain locations (sweet spots) of the matrix-analyte crystals as the traditional matrices were used (Fig.S2A, ESI†). However, Fig.S2B (ESI†) showed a homogeneous Fe_3O_4@ZIF-8-analyte crystal layer that minimized the need to search for sweet spots. Significantly, it avoided the variability of signal intensity across different locations on the target surface due to the heterogeneous crystals and greatly improved spot-to-spot reproducibility. Fig.1D showed a comparison of the MS signals of His as model sample with three different sample preparation procedures (sample-first, matrix-first and dried-droplet methods).[11] No signal was observed with the sample-first method, whereas a deprotonated ion of His with signal-to-noise ratio (S/N) of 33.5 was obtained by using matrix-first method. In contrast, the signal intensity of His obtained by the dried-droplet method was relatively high (S/N=155) as compared to the former two methods. The high ionization efficiency can be attributed to the thorough mixing, which leads to high adsorption. Based on the results, the dried-droplet method was recommended for further studies.

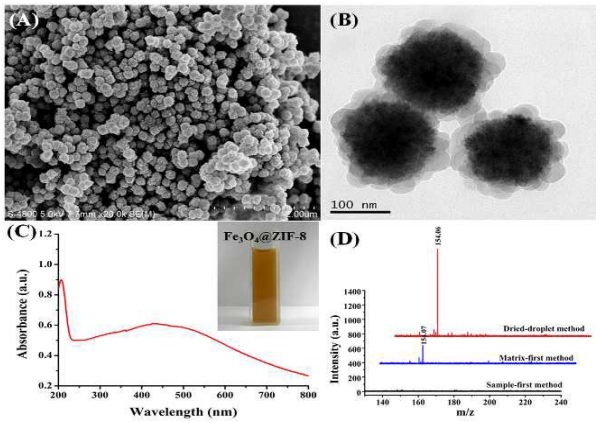

Fig.1 SEM (A) and TEM (B) images of Fe_3O_4@ZIF-8 MNCs; (C) UV-vis spectrum of 1.0 mg mL^{-1} Fe_3O_4@ZIF-8 suspension; (D) Mass spectra of His with different sample preparation methods. (1mM His for sample-/matrix-first method, and 0.5 mM His for dried-droplet method)

For comparison, a mixture of six amino acids was initially analyzed by MALDI-TOF MS using CHCA, 3-aminoquinoline (3-AQ), and Fe_3O_4@ZIF-8 MNCs as matrices in both ion modes. Strong background interferences from the matrices and low S/N ratios of amino acids were obtained with CHCA in positive ion mode (Fig.2A) and 3-AQ in negative ion mode (Fig.2B). However, by using the Fe_3O_4@ZIF-8 MNCs, multiple amino acid-related positive ions in the forms of $[M+Na]^+$, $[M+K]^+$, $[M+2Na-H]^+$, $[M+2K-H]^+$, and $[M+Na+K-H]^+$ ions were observed (Fig.2C and Table S1, ESI†). Apparently, the complicated mass spectra obtained in positive ion mode make it rather difficult for interpretation. In contrast, negative ion mode provides clean background for detection of amino acids and the result was illustrated in Fig.2D, where the characteristic $[M-H]^-$ ions of Asp, Gln, His, Phe, Tyr, and Trp at m/z 132.06, 145.09, 154.09, 164.13, 180.14, and 203.18 predominated the mass spectra. Moreover, the signal intensities of amino acids generated in negative ion mode were much stronger than those obtained in positive ion mode under the same laser energy. The result can stand comparison with those using graphene- and single-walled carbon nanohorns (SWNHs) matrices,[6b-d] but better than those obtained with Pt- and TiO_2-based matrices in the same ion mode,[12] because the latter showed weak adaptability for amino acid analysis.

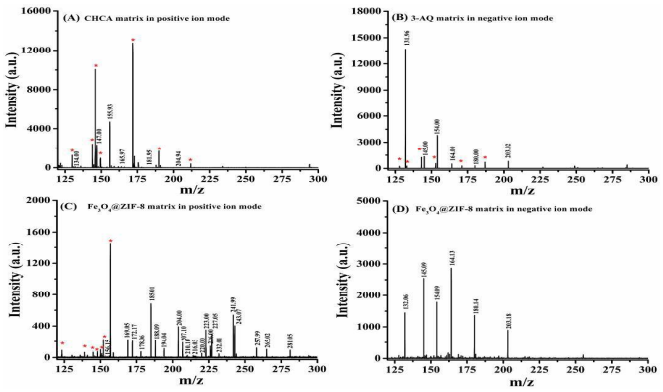

Fig.2 Mass spectra of amino acids by using (A) CHCA matrix in positive ion mode; (B) 3-AQ matrix in negative ion mode; (C) Fe3O4@ZIF-8 MNC matrix in positive ion mode and (D) negative ion mode. The concentration of all analytes was set as 1 mM for CHCA and 3-AQ, but 0.5 mM for Fe3O4@ZIF-8 MNC. Laser intensity: 60%. Red asterisk is background peaks of matrix unless otherwise noted.

To further demonstrate the feasibility of the novel Fe_3O_4@ZIF-8 MNC matrix under robust applications, a wide variety of small molecules were analyzed. It is underscored by the fact that none of the selected fatty acids were detected with CHCA or 3-AQ in either positive- or negative ion mode. However, the exclusive $[M-H]^-$ ions of fatty acids with clean background were obtained using Fe_3O_4@ZIF-8 MNC matrix in negative ion mode (Fig.3A). Fig.3B shows that the Fe_3O_4@ZIF-8 MNC matrix resulted in free matrix interference in the low mass regions, where seven peptides at m/z 215.98, 220.97, 249.11, 327.34, 425.49, 554.53 and 609.00 were well detected, responding to $[Ala-Gln-H]^-$, $[Gly-Phe-H]^-$, $[Tyr-Gly-Gly-2Na]^-$, $[Tyr-Phe-H]^-$, $[Phe-Gly-Phe-Gly-H]^-$, $[Tyr-Gly-Gly-Phe-Leu-H]^-$, and $[Arg-Ser-Gly-Phe-Tyr-H_2O-H]^-$, respectively. In comparison, using CHCA and Fe_3O_4@ZIF-8 MNCs in positive ion mode or 3-AQ in negative ion mode gave rise to complicated alkali metal adducts and serious matrix interference (Fig.S3 and Table S2, ESI†). In addition, the characteristic ions at m/z 271.30, 223.10, and 144.00, assigned to 17β-estradiol (E2, $[M-H]^-$), testosterone (T, $[M-2Na-H_2O-H]^-$) and 8-hydroxyquinoline (8-HQ, $[M-H]^-$) were obtained with

the S/N ratios of 80, 107.5, and 92.8, even at low concentrations of 0.5 mM for each analytes (Fig.3C-E). Although bisphenol A (BPA) was detected in the form of $[M-H]^-$ ion and $[M-CH_3-H]^-$ ion that means a possible rearrangement reaction occurred, high S/N (>500) ratio can be achieved even at a low concentration (0.5 mM) (Fig.3F).

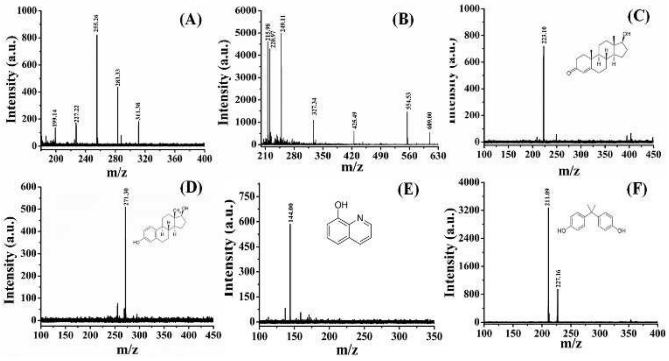

Fig.3 Mass spectra of (A) fatty acids, (B) peptides, (C) E2, (D) T, (E) 8-HQ, and (F) BPA using Fe_3O_4@ZIF-8 MNC in negative-ion mode. (Details was seen in ESI†)

Salt tolerance was investigated and the result (Fig.S4, ESI†) showed that NaCl concentration up to 1000 mM witnessed a slight decline by less than 25% of the initial intensities for the peptides. Nevertheless, the peptides could be unambiguously detected, indicating its good salt tolerance. Fig.S5 (ESI†) showed the signal reproducibilities of His obtained using Fe_3O_4@ZIF-8 MNC matrix. The relative standard deviations (RSDs) for shot-to-shot and sample-to-sample assays were 6.8% (n=15) and 15.1% (n=10), respectively, suggesting that no "sweet spot" problem resulted from the use of Fe_3O_4@ZIF-8 MNC as a matrix.

To investigate the feasibility of Fe_3O_4@ZIF-8 MNC as a matrix for quantitative analysis, melatonin (MT) was selected as a model compound. Fig.S6-S7 (ESI†) represented the quantitative analysis of MT at different concentrations. A linear relationship was found between the MS signals of MT and its concentration in the range of 0.5 to 500 μM (R^2 = 0.9965). Notably, the deprotonated ion of MT could still be detected with S/N ratio of 6.6, even in the case of 0.5 μM (equivalent to 0.5 pmol). The limit of detection (LOD) obtained in the present work is much better than that of the previous work.[12] As presented in Fig.4, no MT was detected in blank serum and urine samples. After spiking MT with 0.5 μM, however, an unambiguous $[M-H]^-$ ion of MT was observed in both samples. Moreover, the signal intensity of MT in the spiked serum or urine was comparable to that in standard test solution, implying its good resistance to the complex substrate of real sample. In addition, the recovery test was conducted and the results were listed in Table S3 (ESI†). Stimulated by the results, it is believed that the Fe_3O_4@ZIF-8 MNC-based SALDI MS can be further broadened to monitor and quantify other small molecules in biological samples.

Because of the unique hosting ability of ZIFs-8 to His-containing compounds,[10b] Fe_3O_4@ZIF-8 MNC may serve as adsorbent for His enrichment from solution. The binding experiment validated that the maximum adsorption capacity of the Fe_3O_4@ZIF-8 MNCs towards His is ~ 5.8 mg g^{-1} (equivalent to 3.74×10^{-5} mol g^{-1}) (Fig.S8, ESI†), which made it possible for trapping trace His in water solution. As expected, the MS signals of His decreased with decreasing concentration of His from 500 to 0.5 μM (Fig.S9-10, ESI†), but 5~7 times higher than those obtained with ZIF-8 MOFs (Fig.S11, ESI†). Nevertheless, the concentration of 0.05 μM His is too low to be detected without enrichment. After enrichment, however, there is an obvious His ion signal in mass spectrum, simply demonstrating the applicability of the Fe_3O_4@ZIF-8 MNC-assisted MALDI MS approach to trace His analysis in real sample.

In conclusion, we have demonstrated the potential of Fe_3O_4@ZIF-8 MNCs as absorbent and matrix for the first time. Compared to organic matrices, the Fe_3O_4@ZIF-8 MNCs exhibited many advantages, including interference-free background, good salt tolerance, high sensitivity and reproducibility in the analysis of small molecules. Besides, the Fe_3O_4@ZIF-8 MNCs can be used as adsorbent to enrich trace His from solution, isolated easily with a magnet, and directly spotted for SALDI-MS, with which sensitive detection of His can be achieved. It is believed that the Fe_3O_4@ZIF-8 MNCs would be an alternative matrix to solve more analytical challenges.

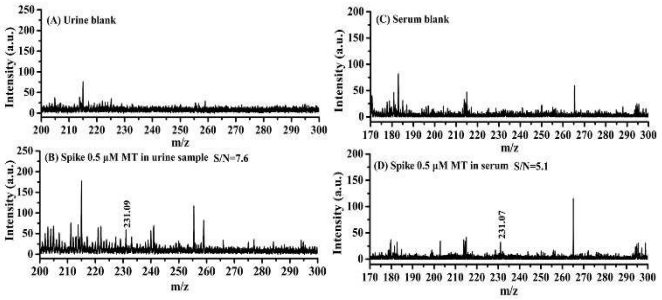

Fig.4 Mass spectra of (A) blank urine; (B) 0.5 μM MT in spiked urine; (C) blank serum; and (D) 0.5 μM MT in spiked serum by using Fe_3O_4@ZIF-8 MNC in negative ion mode. Laser intensity: 60%.

This study was supported by Grant 21375018 and 21175025 from the National Natural Science Foundation of China.

Notes and references

1. (a) K. Tanaka, H. Waki, Y. Ido, S. Akita, S, and Y. Yoshida, *Rapid Commun. Mass Spectrom.* 1988, **2**, 151−153. (b) F. Chen, S. Gerber, K. Heuser, V. M. Korkhover, C. Lizak, S. Mireku, K. P. Locher, and R. Zenobi, *Anal. Chem.* 2013, **85**, 3483−3488.

2. Z. Guo, Q. Zhang, H. Zou, B. Guo, and J. Ni, *Anal. Chem*. 2002, **74**, 1637–1641.

3. J. Sunner, E. Dratz, and Y.C. Chen, *Anal. Chem*. 1995, **67**, 4335−4342.

4. (a) J. Wei, J. M. Buriak, and G. Siuzdak, *Nature* 1999, **399**, 243–246; (b) A. Nordström, J.V. Apon, W. Uritboonthai, E. Go, and G. Siuzdak, *Anal. Chem.* 2006, **78**, 272–278.

5. (a) B.L. Walton, and G.F. Verbeck, *Anal. Chem.* 2014, **86**, 8114–8120; (b) Y.F. Huang, and H.T. Chang, *Anal. Chem*., 2007, **79**, 4852–4859.

6. (a) H. Zhang, S.W. Cha, and E.S. Yeung, *Anal. Chem.* 2007, **79**, 6575–6584.; (b) Q.H. Min, X.X. Zhang, X.Q. Chen, S.Y. Li, and J.J. Zhu, *Anal. Chem.* 2014, 86, 9122–9130.; (c) M.H. Lu, Y.Q. Lai, G.N. Chen, and Z.W. Cai, *Anal. Chem.* 2011, **83**, 3161–3169.; (d) R.N. Ma, M.H. Lu; L. Ding, H.X. Ju, and Z.W. Cai, *Chem. Eur. J.* 2013, **19**, 102-108.

7. C.S. Pan, S.Y. Xu, L.G. Hu, X.Y. Su, J.J. Ou, H.F. Zou, Z. Guo, Y. Zhang, and B.C. Guo, *J. Am. Soc. Mass Spectrom*. 2005, **16**, 883−892.; (d) R.N. Ma, M.H. Lu; L. Ding, H.X. Ju, and Z.W. Cai, *Chem. Eur. J.* 2013, **19**, 102-108.

8. (a) Y.Y. Fu, C.X. Yang, and X.P. Yan, *Chem. Commun.,* 2013,**49**, 7162-7164.; (b) C.L. Chang, X.Y. Qi, J.W. Zhang, Y.M. Qiu, X.J. Li, X. Wang, Y. Bai, J.L. Sun and H.W. Liu, *Chem. Commun.,* 2015, **51**, 3566-3569.; (c) Y.H. Shih, C.H. Chien, B. Singco, C.L. Hsu, C.H. Lin, and H.Y. Huang, *Chem. Commun.,* 2013, **49**, 4929–4931.

9. (a) R. Banerjee, A. Phan, B.Wang, C. Knobler, H. Furukawa, M. O'Keeffe, and O.M. Yaghi, *Science*, 2008, **319**, 939–943.; (b) G, Lu, and J.T. Hupp, *J. Am. Chem. Soc.,* 2010, **132**, 7832–7833.

10. (a) J. Zheng, C. Cheng, W.J. Fang, C. Chen, W.R. Yan, H.X. Huai, and C.C. Wang,

CrystEngComm, **2014**, 16, 3960–3964.; (b) J.N. Zheng, Z.A. Lin, G. Lin, H.H. Yang, and L. Zhang, *J. Mater. Chem. B*, 2015, **3**, 2185–2191.

11. (a) S. Nitta, H. Kawasaki, T. Suganuma, Y. Shigeri, and R. Arakawa, *J. Phys. Chem. C* 2013, **117**, 238−245.; (b) H. Sonderegger, H. Rameshan, H. Lorenz, F. Klauser, M. Klerks, M. Rainer, R. Bakry, C.W. Huck, and G.K. Bonn, *Anal. Bioanal. Chem*. 2011, **401**, 1963–1974.

12. G. Chen, X.G. Ding, Z.G. Cao, and J.N. Ye, *Anal Chim Acta* 2000, **408**, 249–256.

